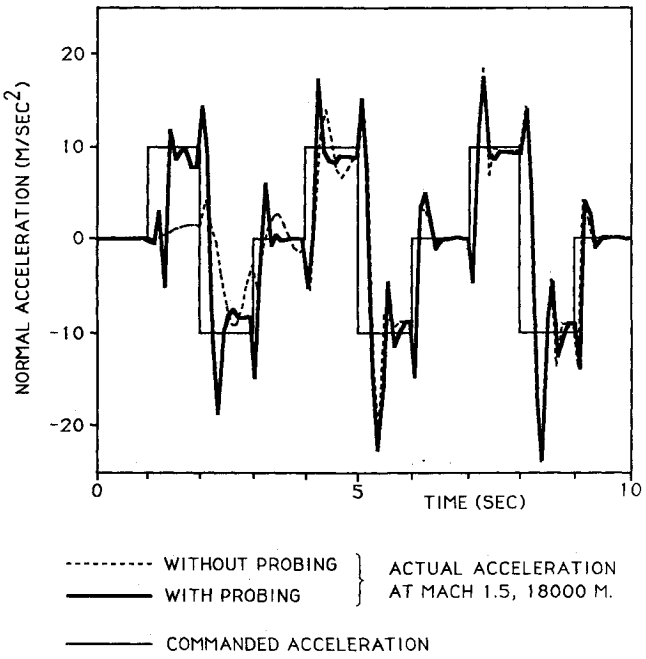

Fig. 1 Autopilot response in a realistic computer simulation of missile and aerodynamics.

case when implemented judiciously. This example is an adaptive missile autopilot[3,4] where the controller measures the missile's acceleration normal to the flight path and seeks to make it follow a commanded acceleration by rotating the missile with tail-fin deflections (the control variable) to create body lift. Instead of being limited by established theory, the prior variances of the (two) unnormalized parameters, which are proportional to h^2 and reflect variability in the flight conditions, were made as large as would empirically allow reasonable behavior at the nominal flight condition, which is Mach 2.0 at 6000 m altitude. The probing control term has little effect then but substantially improves the initial performance for the very different flight condition of Fig. 1 by causing the parameter estimates to converge more quickly to the corresponding nonzero values, which occurs because this control term reduces the uncertainties of these parameters more quickly.

Conclusions

Asymptotic approximations of optimal control laws have been established for a class of dynamic systems whose state components are either slowly varying (i.e., parameters) or can be tracked arbitrarily well by making the controller's measurements sufficiently accurate. These control optimization problems have the form assumed by higher order descriptions of noise-induced perturbations from optimal nominal behavior in a more general type of control problem. When the measurement noise is small, bilinear measurement terms in the parameter and control variables can give rise to a rapidly fluctuating "probing" term in the optimal control. This term is the output of a high-frequency linear system driven by a product of the parameter covariance matrix and a Kalman filter innovation vector.

References

[1]Bryson, A. E., and Ho, Y.-C., *Applied Optimal Control,* Hemisphere, Washington, DC, 1975, Chap. 14.

[2]Willman, W. W., "Some Formal Effects of Nonlinearities in Optimal Perturbation Control," *Journal of Guidance and Control,* Vol. 2, No. 2, 1979, pp. 99-100.

[3]Willman, W. W., "Probing Behavior in Certain Optimal Perturbation Control Laws," Naval Weapons Center, TP 7081, China Lake, CA, July 1990.

[4]Willman, W. W., "Optimal Control Law Phenomena in Certain Adaptive Second-Order Observation Systems," Naval Weapons Center, TP 7030, China Lake, CA, Aug. 1989.

[5]Feldbaum, A. A., "Dual Control Theory I," *Automation and Remote Control,* Vol. 21, No. 9, 1961, pp. 874-889.

[6]Bar-Shalom, Y., "Stochastic Dynamic Programming: Caution and Probing," *IEEE Transactions on Automatic Control,* Vol. AC-26, Oct. 1981, pp. 1184-1195.

Deployment of a Flexible Beam from an Oscillating Base

Nelson G. Creamer*
Swales and Associates, Inc.,
Beltsville, Maryland 20705

Introduction

MANY past, present, and future spacecraft employ long flexible appendages that must be launch-stored for compactness and subsequently deployed in orbit. An extensive amount of research and analysis has been directed toward the dynamics associated with deployment of flexible appendages from both a fixed base and a host spacecraft (see, for example, Refs. 1-5). To this date, however, very little analysis has focused on the dynamic interaction of a flexible appendage and its deployment mechanism, which, as observed during deployment and retraction of the Shuttle-based solar array flight experiment (SAFE), may result in large flexural deformations and possible damage to the deploying boom.[6] These structural deformations are attributed to a resonant interaction of the instantaneous appendage natural frequencies and a slight oscillatory motion within the deployment mechanism. The objective of this Note is to examine this resonant interaction using Timoshenko beam theory in conjunction with base oscillatory motion.

Governing Equations

The system of interest is a flexible beam with a tip payload that is axially deployed from a fixed canister, as shown in Fig. 1. Internal to the canister is a motor-driven rotating system that uncoils and deploys the appendage. This rotating mechanism produces a small periodic translational motion $[\delta(t)]$ and a small periodic rotational motion $[\gamma(t)]$ of the base of the appendage. An internal view of a typical canister, similar to the ones used on the SAFE experiment and the Naval Research Laboratory's Low-power Atmospheric Compensation Experiment (LACE), is shown in the enlargement of Fig. 1. It is observed that there are three regions of interest: 1) a storage region where a truss structure is coiled and stored; 2) a turntable region that rotates at a prescribed frequency, thereby uncoiling the truss; and 3) an elevating region in which nuts and rails are used to guide and deploy the truss as it uncoils. It is in this third region that the base motion can occur due to an interaction of the rotating, uncoiling truss structure with slight freeplay in the roller system.

Lagrange's equations are used to derive the equations of motion for the system. The potential energy can be written in the form

$$V = \frac{1}{2}\int_0^L \left[EI\left(\frac{\partial \alpha}{\partial x}\right)^2 + \kappa GA\left(\alpha - \frac{\partial v}{\partial x}\right)^2 \right] dx \qquad (1)$$

Presented as Paper 90-1239 at the AIAA Dynamics Specialist Conference, Long Beach, CA, April 5-6, 1990; received July 20, 1990; revision received Nov. 1, 1990; accepted for publication Nov. 8, 1990.

*Engineer. Member AIAA.

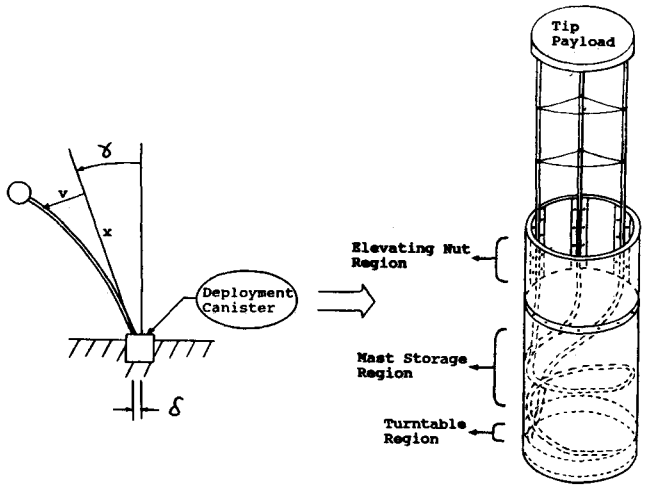

Fig. 1 Deployment system configuration.

where α is the rotation of a segment along the beam, v the transverse displacement of a segment along the beam, EI the beam bending stiffness, GA the beam shear stiffness, and κ the shear correction factor. The kinetic energy can be written in the form

$$T = \frac{1}{2}\int_0^L \rho \dot{r}_{dm} \cdot \dot{r}_{dm}\, dx + \left(\frac{1}{2}\right)\int_0^L I_z w_z^2\, dx + \left(\frac{1}{2}\right) m_T \dot{r}_T \cdot \dot{r}_T + \left(\frac{1}{2}\right) I_{zT} w_{zT}^2 \tag{2}$$

where $\dot{r}_{dm}$ is the velocity vector of a segment along the beam, $w_z\,(=\dot{\gamma}+\dot{\alpha})$ the angular velocity of a segment along the beam, ρ the beam mass/length, I_z the beam rotational inertia/length, m_T the payload mass, and I_{zT} the paylod rotational inertia. To discretize the equations, the beam displacement and rotation functions are expanded in the form

$$v(x,t) = \sum_{i=1}^{m} q_i(t)\psi_i[x, L(t)] \tag{3a}$$

$$\alpha(x,t) = \sum_{i=1}^{n} s_i(t)\phi_i[x, L(t)] \tag{3b}$$

where q_i and s_i are the ith unknown generalized coordinates, and ψ_i and ϕ_i are the ith prescribed beam shape functions that satisfy the geometric boundary conditions. It is clear that Eqs. (3) are not the rigorously classical assumed-modes method; however, the expansion is valid as long as the beam length does not change rapidly during an integration step (see Refs. 3 and 4 for further applications of this approach). Defining the $(m+n)$ vector z as $z^T = \{q_1 q_2 \ldots, s_1 s_2 \ldots\}$ and incorporating Eqs. (3) into Eqs. (1) and (2) yields the following general expressions for the system energy:

$$T = (\tfrac{1}{2})[\dot{z}^T M \dot{z} + 2z^T B\dot{z} + z^T D z + f^T z + g^T \dot{z}] \tag{4a}$$

$$V = (\tfrac{1}{2})[z^T K z] \tag{4b}$$

Definitions of the matrices that appear in Eqs. (4) are provided in the Appendix. By assuming that the unknown beam motion and the prescribed base motion are small quantities, the linearized transverse equations of motion now follow from application of Lagrange's equations, resulting in the system form

$$[M]\ddot{z} + [\dot{M} + B^T - B]\dot{z} + [\dot{B}^T - D + K]z = (\tfrac{1}{2})\{f - \dot{g}\} \tag{5}$$

Example Application

The transverse motion of an axially deploying truss boom is examined to compare theory with experiment. The representative boom is one similar to those flying on the LACE spacecraft and has the following approximate characteristics:

$$EI = 5.28 \times 10^7 \text{ slug-in.}^3/\text{s}^2$$

$$\kappa GA = 1.8 \times 10^5 \text{ slug-in./s}^2$$

$$\rho = 5.28 \times 10^{-4} \text{ slug/in.}$$

$$I_z = 0.02 \text{ slug-in.}^2/\text{in.}$$

$$m_T = 1.242 \text{ slug}$$

$$I_{zT} = 300.0 \text{ slug-in.}^2$$

$$\dot{L} = 3.0 \text{ in./s}$$

$$\delta(t) = 0.05\cos(2\pi t) \text{ in.}$$

$$\gamma(t) = 0.0$$

The base motion is chosen to match a 1-Hz driving frequency of the rotating turntable inside the deployment canister.

Simulated results for the tip acceleration and root bending moment are provided in Figs. 2a and 2b. In this simulation, the shape functions were chosen to be simple polynomials, wherein convergence occurred with three terms in the series. The resonant condition that occurs at a length of 165 in. is due to the interaction of the beam fundamental mode with the base shaking mode of 1 Hz. The root bending moment history exemplifies the potentially large bending moments that can occur near resonance for a deployment system of this type.

Deployment experiments for the LACE booms were conducted at the ABLE Engineering Company in Santa Barbara, California, prior to launch. The boom was deployed from the canister in a horizontal plane and supported with a bungee cord (connected to a traveler on the ceiling of the building) to offset gravity. Accelerometers attached to the tip mass provided results such as that shown in Fig. 2c. It is observed that there are two noticeable resonances that occur when the boom has been deployed about 92 and 48 in. Fixed-length twang tests revealed that these two lengths exhibited fundamental natural frequencies of 1 and 2 Hz, respectively, implying that the base

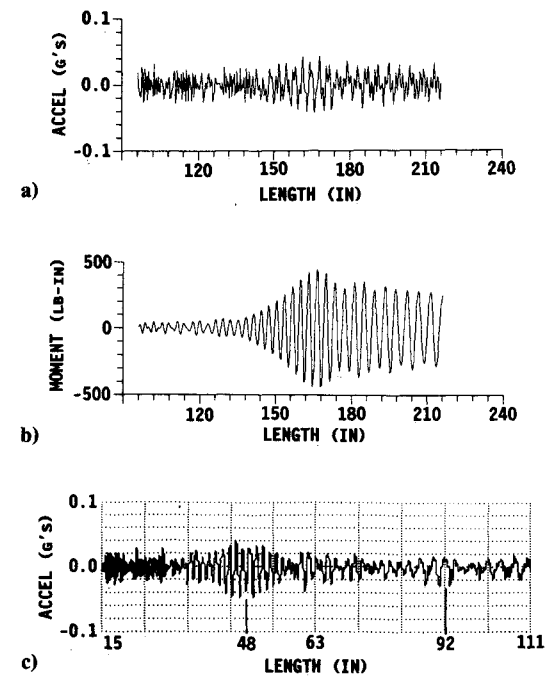

Fig. 2 Results for a) simulated acceleration history, b) simulated bending moment history, and c) experimental acceleration history.

was likely being driven by the canister turntable frequency and its first multiple. Although there is clear qualitative agreement between theory and experiment, the theoretical resonance occurred at a longer boom length than the experiment (165 vs 92 in.). It is believed that this difference is due to the representation of a complex joint-dominated truss structure by a Timoshenko beam with uniform properties and perfect boundary conditions. Although a modification of the properties of the beam could be attempted to more accurately match the experimental results, such an effort was not performed in this study.

Summary

The deployment of a flexible boom from an oscillating base may result in potentially large resonant-driven bending moments that can be detrimental to the boom structure. In systems such as the one studied here, the base oscillation, due to interaction of a rotating turntable device with slight freeplay within the deployment canister, should be characterized experimentally prior to flight to ensure boom health.

Appendix: Matrix Definitions

If z is defined as $z^T = \{q_1 q_2 \ldots, s_1 s_2 \ldots\} = \{z_1, z_2\}$, the definitions of the nonzero elements of the matrices appearing in the transverse equations of motion are given as the following:

$$M_{11ij} = \int_0^L \rho \psi_i \psi_j \, dx + m_T \psi_{iL} \psi_{jL}$$

$$M_{22ij} = \int_0^L I_z \phi_i \phi_j \, dx + I_{zT} \phi_{iL} \phi_{jL}$$

$$B_{11ij} = \int_0^L \rho \dot{\psi}_i \psi_j \, dx + m_T \dot{\psi}_{iL} \psi_{jL}$$

$$B_{22ij} = \int_0^L I_z \dot{\phi}_i \phi_j \, dx + I_{zT} \dot{\phi}_{iL} \phi_{jL}$$

$$D_{11ij} = \int_0^L \rho \dot{\psi}_i \dot{\psi}_j \, dx + m_T \dot{\psi}_{iL} \dot{\psi}_{jL}$$

$$D_{22ij} = \int_0^L I_z \dot{\phi}_i \phi_j \, dx + I_{zT} \dot{\phi}_{iL} \phi_{jL}$$

$$f_{1i} = 2 \int_0^L \rho \left[-\dot{L} \dot{\gamma} \psi_i + (\dot{\delta} + \dot{\gamma} x) \dot{\psi}_i \right] dx + 2 m_T \left[-\dot{L} \dot{\gamma} \psi_{iL} + (\dot{\delta} + \dot{\gamma} L) \dot{\psi}_{iL} \right]$$

$$f_{2i} = 2 \int_0^L I_z \dot{\gamma} \dot{\phi}_i \, dx + 2 I_{zT} \dot{\gamma} \dot{\phi}_{iL}$$

$$g_{1i} = 2 \int_0^L \rho (\dot{\delta} + \dot{\gamma} x) \psi_i \, dx + 2 m_T (\dot{\delta} + \dot{\gamma} L) \psi_{iL}$$

$$g_{2i} = 2 \int_0^L I_z \dot{\gamma} \phi_i \, dx + 2 I_{zT} \dot{\gamma} \phi_{iL}$$

$$K_{11ij} = \int_0^L \kappa G A \left(\frac{\partial \psi_i}{\partial x} \right) \left(\frac{\partial \psi_j}{\partial x} \right) dx$$

$$K_{12ij} = -\int_0^L \kappa G A \left(\frac{\partial \psi_i}{\partial x} \right) \phi_j \, dx = K_{21ji}$$

$$K_{22ij} = \int_0^L \left[EI \left(\frac{\partial \phi_i}{\partial x} \right) \left(\frac{\partial \phi_j}{\partial x} \right) + \kappa G A \phi_i \phi_j \right] dx$$

References

[1]Barakat, R., "Transverse Vibrations of a Moving Thin Rod," *Journal of the Acoustical Society of America,* Vol. 43, No. 3, 1968, pp. 533–539.

[2]Cherchas, D. B., "Dynamics of Spin-Stabilized Satellites During Extension of Long Flexible Booms," *Journal of Spacecraft and Rockets,* Vol. 8, No. 7, 1971, pp. 802–804.

[3]Tabarrok, B., Leech, C. M., and Kim, Y. I., "On the Dynamics of an Axially Moving Beam," *Journal of the Franklin Institute,* Vol. 297, No. 3, 1974, pp. 201–220.

[4]Lips, K. W., and Modi, V. J., "Three-Dimensional Response Characteristics for Spacecraft with Deploying Flexible Appendages," *Journal of Guidance and Control,* Vol. 4, No. 6, 1981, pp. 650–656.

[5]Banerjee, A. K., and Kane, T. R., "Extrusion of a Beam from a Rotating Base," *Journal of Guidance, Control, and Dynamics,* Vol. 12, No. 2, 1989, pp. 140–146.

[6]Slaby, J.,"Evaluation of Solar Array Flight Experiment Response During Flight for Extension/Retraction Phase," NASA TM-86551, June 1986.

Eigenstructure Assignment for the Extended Medium Range Air-to-Air Missile

Kenneth Sobel*
City College of New York, New York, New York 10031
and
James R. Cloutier†
U.S. Air Force Wright Laboratories, Eglin Air Force Base, Florida 32542

Introduction

EIGENSTRUCTURE assignment is applied to the design of an autopilot for the extended medium range air-to-air technology (EMRAAT) missile. We compute eigenstructure assignment feedback gains by choosing desired eigenvectors based on mode decoupling and using the orthogonal projection solution suggested by Andry et al.[1] to compute achievable eigenvectors. We compare our solution to the linear quadratic regulator design that was proposed by Bossi and Langehough.[2] An important difference between this application and other eigenstructure assignment applications that have appeared in the literature is that the lateral dynamics of the EMRAAT missile does not have a well-defined Dutch roll mode. Therefore, eigenstructure assignment is utilized not only for mode decoupling, but also to create distinctly separate Dutch roll and roll modes.

Eigenstructure Assignment

Consider a linear time-invariant multi-input multi-output system described by the triple (A,B,C). The eigenstructure assignment problem was considered by Andry et al.[1] who have shown the need for the eigenvector v_i to be in the subspace spanned by the columns of $(\lambda_i I - A)^{-1}B$. In general, however, a desired eigenvector v_i^d will not reside in the prescribed subspace and, hence, cannot be achieved. Instead, it is suggested in Ref. 1 that an achievable eigenvector be chosen as the projection of v_i^d onto the subspace that is spanned by the columns of $(\lambda_i I - A)^{-1}B$.

Missile Autopilot Design

Consider the EMRAAT bank-to-turn missile, which is described by Bossi and Langehough.[2] A sixth-order model of the yaw/roll dynamics at a 10-deg angle of attack is con-

Received Oct. 29, 1990; revision received Jan. 8, 1991; accepted for publication Feb. 22, 1991. This paper is declared a work of the U.S. Government and is not subject to copyright protection in the United States.

*Associate Professor, Department of Electrical Engineering. Associate Fellow AIAA.

†Technical Advisor, Guidance and Controls Branch, WL/MNAG. Associate Fellow AIAA.